Micro/magnetic structural development in Co-Ni-Cr and Co-Ni-Cr/Cr films for longitudinal recording media

J.-W. Lee, K. R. Mountfield, and D. E. Laughlin
Department of Metallurgical Engineering and Materials Science and Magnetics Technology Center, Carnegie Mellon University, Pittsburgh, Pennsylvania 15213

A series of Co-Ni-Cr and Co-Ni-Cr/Cr films have been examined using transmission electron microscopy in conventional bright/dark-field imaging, selected-area diffraction, convergent beam electron diffraction, as well as in Lorentz electron microscopy imaging mode. The crystallographic orientation and magnetic domain structure have been characterized as a function of film thickness. The results indicate that amorphous Co-Ni-Cr films form prior to the formation of small randomly oriented equiaxed grains during deposition on amorphous substrates. As the film thickness increases, some of the small grains grow preferentially with their c axis parallel to film plane, but others with their c axis at an angle of 62° from the film plane. Longitudinal domain structures of the films were found to consist of Néel walls associated with cross-tie walls and Bloch lines. Each domain contains a large amount of the magnetic ripple-type structure.

INTRODUCTION

Co-Ni-Cr/Cr films are promising candidates for high-density longitudinal recording media. One material requirement for high recording density is that the crystals of the media have their c axes parallel to the film plane.[1,2] The bilayer film of Co-Ni-Cr/Cr has been suggested to fulfill this requirement. It is thought that these films will form with the desired crystal texture when grown epitaxially on a {110} textured Cr underlayer. However, the {110} planes of Cr are found to give rise to the epitaxial formation of the $\{01\bar{1}1\}$ planes of Co-Ni-Cr.[3,4] Films with these planes parallel to the substrate show higher in-plane coercivity (H_c) than the ones with $\{10\bar{1}0\}$ planes[3] although the opposite has been confirmed in Co-Ni films.[2] Few of the published papers for Co-Ni, Co-Ni-Cr, and Co-Ni-Cr/Cr films have correlated microstructures with the corresponding magnetic domain structures.[5] Thus, the objectives of this investigation are to study the microstructural details of the films and analyze their crystallography utilizing convergent beam electron diffraction (CBED) as well as to examine the relation between magnetic domain structure and microstructure.

EXPERIMENT

The Co-Ni-Cr, Co-Ni-Cr/Cr, and Cr films were prepared from an alloy target of 62.5Co-30Ni-7.5Cr(at. %) and a pure Cr target by an rf sputtering system. The films were deposited on carbon-coated copper grids for direct transmission electron microscopy (TEM) observation.[6] The deposition conditions were held constant; the deposition rate was 9.6 nm/min. Microstructural details were obtained by TEM using a Philips EM420T analytical electron microscope. The magnetic domain observations were carried out by Fresnel mode imaging in Lorentz electron microscopy (LEM).

RESULTS AND DISCUSSIONS

CBED patterns of all the films showed that they contain a predominantly hcp structure. Occasionally, fcc structures have been detected. Figure 1 is a typical bright-field TEM micrograph (a) of a 5.0-nm film together with its dark-field image (b), selected area diffraction (SAD) (c), and CBED patterns (d). Figure 1(a) shows that the microstructure of a Co-Ni-Cr film is mainly amorphous with a small number of isolated crystalline grains (see arrow). Honeycomblike networks associated with microvoids can be observed.[6] The existence of crystalline grains within an amorphous matrix can be confirmed by a dark-field image using the first ring of the SAD pattern. The crystal size is shown to be less than 4.5 nm. It should be noted, however, that the SAD pattern shows two additional diffuse rings of very low intensity. In contrast, the CBED pattern exhibits sharp crystalline reflections from fine grains superimposed on the intense ring from the amorphous phases. The initial formation of the amorphous phase is similar to the previously reported result on Co-Cr films.[6]

As the film thickness increases to 10 nm, the amount of amorphous phase decreases drastically with a corresponding increase in the number of crystalline Co-Ni-Cr grains [Fig. 2(a)(2)]. At this thickness, the structure shows a larger honeycomblike network of the crystalline phases [Fig. 2(a)

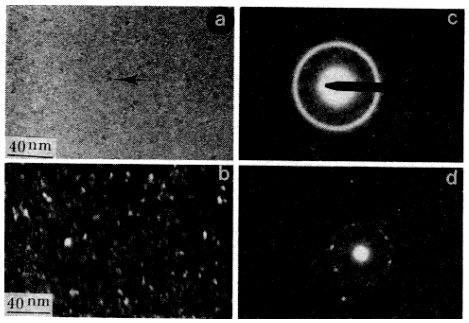

FIG. 1. TEM images of 5.0-nm-thick Co-Ni-Cr film on a carbon-coated Cu grid in bright field (a) and in dark field (b), together with SAD (c) and CBED (d) patterns.

 0021-8979/88/083266-03$02.40 © 1988 American Institute of Physics

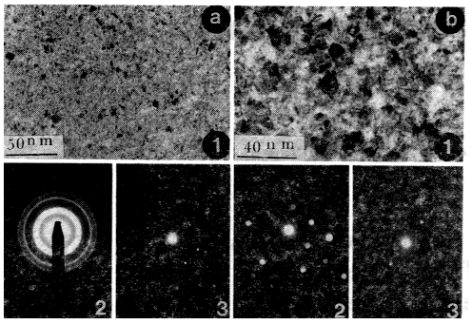

FIG. 2. Bright-field TEM images (1) of Co-Ni-Cr films on a carbon-coated Cu grid together with their representative SAD [(a)(2)] and CBED [(a)(3), (b)(2), and (b)(3)] patterns; (a) 10 nm thick and (b) 30 nm thick.

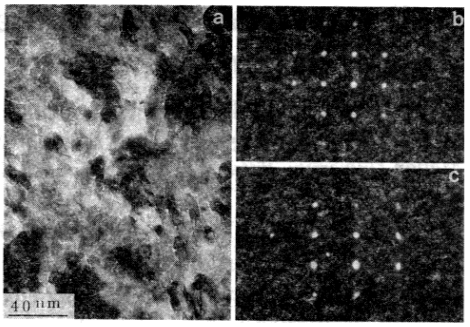

FIG. 4. A TEM image (a) of Cr film on a carbon-coated Cu grid together with its representative CBED patterns [(b) and (c)] (b) $z = [001]$ and (c) $z = [110]$.

(1)]. The grain size is very small (< 6.8 nm). Thus, the CBED patterns are halolike patterns composed of a superposition of many $(01\bar{1}0)$ and $(01\bar{1}1)$ reflections [Fig. 2(a)(3)].

As the film thickness increases even further (30 nm), the honeycomblike networks disappear [Fig. 2(b)(1)] and the grain size is in the range of 6–11 nm. The grains are still randomly oriented. Relatively low index zone axes such as [0001] [Fig. 2(b)(2)], $[1\bar{2}1\bar{3}]$ [Fig. 2(b)(3)], $[01\bar{1}0]$, $[01\bar{1}1]$, and $[5\bar{1}\bar{4}3]$ were frequently encountered.

In the 50-nm thickness film (Fig. 3), the grain size is in the range of 10–15 nm, much larger than that for thinner films (< 4.5 nm at 5.0 nm thickness). Additionally, Moiré fringes are frequently observed in the grains [arrow, Fig. 3(a)]. Both the difference in grain size and the observation of Moiré fringes indicate that the film grows in the form of laterally expanding conical columns.[7] CBED results show that the films for this thickness are composed of less randomly oriented grains than the thinner films. The $[01\bar{1}1]$ [Fig. 3(b)] and $[01\bar{1}0]$ [Fig. 3(c)] zone axes are frequently observed with less frequent occurrence of [0001] or $[1\bar{2}1\bar{3}]$ zone axes. The small amount of fcc structure does not disappear with increasing thickness as shown in Fig. 3(d) ($z = [001]$).

Figure 4 shows a bright-field image of a 50-nm Cr film on a carbon-coated copper grid, together with its representative CBED patterns. The film shown in Fig. 4(a) contains both elongated and equiaxed grains as well as a large number of microvoids present along most of the grain boundaries and grain edges. The formation mechanism of elongated grains and microvoids has been described for Co-Cr films.[6] The representative CBED patterns exhibit [001] [Fig. 4(b)] and [110] [Fig. 4(c)] zone axes. The [001] zone axes are more frequently observed than the [110] zone axes.

Figure 5 represents the magnetic domain structures of Co-Ni-Cr films. In Fig. 5(a) (5.0 nm thick), the magnetic domains are composed of typical Néel-type walls together with twisted magnetic domains (arrow 1) and black and white dots (arrow 2). There is also a slight indication of the formation of cross-tie walls on some of the domain boundaries (arrow 3). In addition, one can see low-angle ripple-type structures within the domains. This observation is not unexpected since the corresponding microstructure exhibits very small randomly oriented grains associated with microvoids within an amorphous matrix [Fig. 1(a)]. The ripplelike structure was frequently observed in randomly oriented Co-Cr thin films[8,9] and even in amorphous thin films.[10]

As the film thickness increases (10 nm), the black and white Néel walls become sharper [Fig. 5(b)]. Also, the ripple contrast is more intense, becoming "featherlike." Increasing film thickness even further (30 nm) [Fig. 5(c)] reveals that most domain boundaries contain the well-

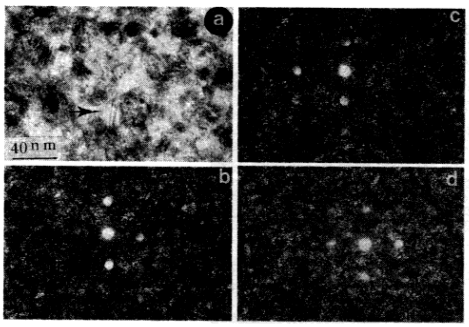

FIG. 3. A TEM image (a) of 50-nm-thick Co-Ni-Cr film on a carbon-coated Cu grid together with its representative CBED patterns [(b), (c), and (d)]; (b) $z = [01\bar{1}1]$, (c) z $[01\bar{1}0]$ for hcp, and (d) $z = [001]$ for fcc.

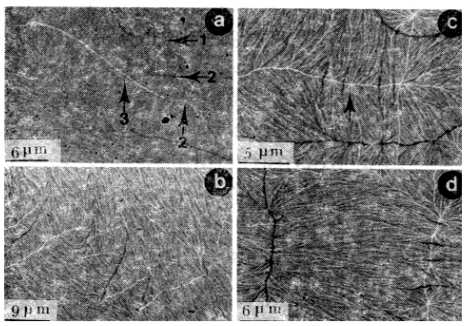

FIG. 5. Lorentz images of Co-Ni-Cr films on a carbon-coated Cu grid; (a) 5.0 nm thick, (b) 10 nm thick, (c) 30 nm thick, and (d) 50 nm thick.

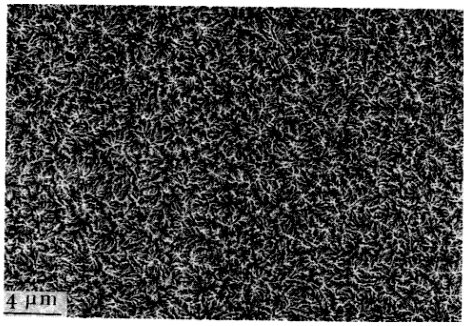

FIG. 6. A Lorentz image of Co-Ni-Cr/Cr film on a carbon-coated Cu grid; 20-nm thickness for Co-Ni-Cr and Cr, respectively.

known cross-tie walls together with Bloch lines (arrow). The featherlike branches are radially distributed from each of the Bloch lines as previously shown in permalloy films.[11]

Films which are 50 nm thick [Fig. 5(d)] exhibit sharper domain wall contrast. The density of cross-tie walls and Bloch lines increases as the film thickness increases. In addition, the featherlike contrast increases. At 50 nm, the films contain predominantly $[01\bar{1}0]$ and $[01\bar{1}1]$ zone axes. These two textures give rise to the strong contrast of the featherlike configuration.

For Co-Ni-Cr/Cr films, no amorphous phase is observed, and the initial grain size mimicks that of the Cr underlayer.[7] The domain configurations are different than those of the Co-Ni-Cr film (Fig. 6) in that the size of domains is smaller and the featherlike contrast is in the shape of a vortex. It is highly likely that magnetostriction contributes to the change in morphology since the epitaxial growth of Co-Ni-Cr on Cr is accompanied by misfit strains.

CONCLUSIONS

(1) An amorphous phase forms in the initial layers of Co-Ni-Cr films mimicking the amorphous substrate. This is followed by the growth of randomly oriented grains and the competitive growth of either $(01\bar{1}0)$ or $(01\bar{1}1)$ films.

(2) The growth of the films may occur by lateral expansion in the form of conical shape along either $\langle 01\bar{1}0\rangle$ or $\langle 01\bar{1}1\rangle$ directions.

(3) Grains of the fcc Co-Ni-Cr phase are occasionally observed.

(4) Thin Cr films show well-oriented grains with {001} zone axis. The structure is composed of equiaxed and elongated grains associated with microvoids.

(5) The magnetic structures are composed of Néel-type walls associated with cross-tie walls and Bloch lines. Each domain includes featherlike configurations.

(6) Twisted magnetic domains have been observed in the Co-Ni-Cr films.

ACKNOWLEDGMENTS

This research was funded in part by the Magnetics Technology Center, Carnegie Mellon University, Pittsburgh, PA 15213, and also supported by the Magnetic Materials Research Group at CMU, through the Division of Materials Research, National Science Foundation, under grant No. DMR-8613386.

[1]T. Chen, D. A. Rogowski, and R. M. White, J. Appl. Phys. **49**, 1816 (1978).
[2]L. F. Herte and A. Lang, Jr., J. Vac. Sci. Technol. **18**, 153 (1981).
[3]G.-L. Chen, IEEE Trans. Magn. **MAG-22**, 334 (1986).
[4]T. Ohno, Y. Shiroishi, S. Hishiyama, H. Suzuki, and Y. Matsuda, INTERMAG 1987, Tokyo, Japan [IEEE Trans. Magn. (in press)].
[5]J. Endo, S. Murakami, S. Fujii, Y. Igarashi, S. Oguma, H. Harada, Y. Ichinose, and T. Ishiguor, *ibid.*
[6]J.-W. Lee, B. G. Demczyk, K. R. Mountfield, and D. E. Laughlin, *ibid.*
[7]J.-W. Lee, B. Wong, and D. E. Laughlin (unpublished).
[8]P. J. Grundy and M. Ali, J. Magn. Magn. Mater. **40**, 154 (1983).
[9]H. Hoffmann, H. Mandl, and T. R. Schurmann, J. Magn. Magn. Mater. **59**, 156 (1986).
[10]L. Rabenberg, R. M. Mishra, G. Thomas, O. Kohomoto, and T. Ojima, IEEE Trans. Magn. **MAG-16**, 1135 (1980).
[11]L. J. Schwee and J. K. Watson, IEEE Trans. Magn. **MAG-9**, 551 (1973).